

Contact mechanics and elements of tribology

Lecture 5.

Micromechanical contact: mechanics

Vladislav A. Yastrebov

MINES ParisTech, PSL University, Centre des Matériaux, CNRS UMR 7633, Evry, France

@ Centre des Matériaux
February 26, 2020

Outline

1 True contact area

How does it grow with the squeezing force?

2 Interfacial fluid flow

How does the permeability decay with the squeezing force?

3 Conclusions & perspectives

How physical are the assumptions and results?

Objective:

link **roughness** parameters with the evolution of the true **contact area** and interface **permeability** with external pressure.

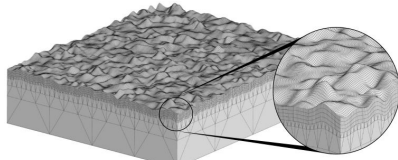
Contact between rough surfaces

Problem

- Solve contact problem for two elastic half-spaces E_1, ν_1 and E_2, ν_2
- With surface roughnesses $z_1(x, y)$ and $z_2(x, y)$
- Balance of momentum $\nabla \cdot \underline{\sigma} = 0$,
- Boundary conditions $-\sigma_z^\infty = p_0$
- Contact constraints $g \geq 0, \quad p \geq 0, \quad g p = 0$,
where $g(x, y)$ is the gap between surfaces,
 $p = -\underline{n} \cdot \underline{\sigma} \cdot \underline{n}$ is the contact pressure.

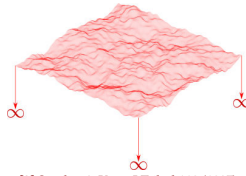
Methods

- Finite element method



[1] Yastrebov, Wiley/ISTE (2013)

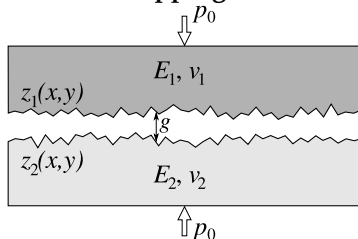
- Boundary element method



[2] Stanley & Kato, J Tribol 119 (1997)

Mapping

Problem mapping



- **Flat** elastic^[1] half-space with $E^* = \frac{E_1 E_2}{E_2(1 - \nu_1^2) + E_1(1 - \nu_2^2)}$
- **Rough** rigid^[1] surface with $z^* = z_2 - z_1$
- Optimization problem^[2]: $\min \mathcal{F}$

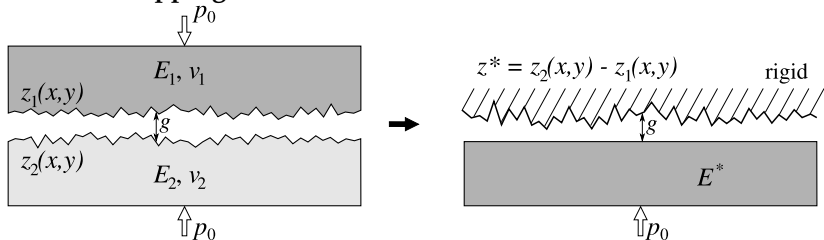
under constraints $p \geq 0$ and $\frac{1}{A_0} \int_A p dA = p_0$,

with $\mathcal{F} = \int_A p[u_z/2 + g]dA$

[1] Barber, Bounds on the electrical resistance between contacting elastic rough bodies, PRSL A 459 (2003)
[2] Kalker, Variational Principles of Contact Elastostatics, J Inst Maths Applies (1977)

Mapping

Problem mapping



- **Flat elastic^[1]** half-space with $E^* = \frac{E_1 E_2}{E_2(1 - v_1^2) + E_1(1 - v_2^2)}$
- **Rough rigid^[1]** surface with $z^* = z_2 - z_1$
- Optimization problem^[2]: $\min \mathcal{F}$

under constraints $p \geq 0$ and $\frac{1}{A_0} \int_A p dA = p_0$,

$$\text{with } \mathcal{F} = \int_A p[u_z/2 + g]dA$$

[1] Barber, Bounds on the electrical resistance between contacting elastic rough bodies, PRSL A 459 (2003)
[2] Kalker, Variational Principles of Contact Elastostatics, J Inst Maths Applies (1977)

Analytical models

Asperity based models

- [1] Greenwood, Williamson. *P Roy Soc Lond A Mat* (1966)
- [2] Bush, Gibson, Thomas. *Wear* (1975)
- [3] Mc Cool. *Wear* (1986)
- [4] Thomas. *Rough Surfaces* (1999)
- [5] Greenwood. *Wear* (2006)
- [6] Carbone. *J. Mech. Phys. Solids* (2009)
- [7] Ciavarella, Greenwood, Paggi. *Wear* (2008)

Persson's model

- [8] Persson. *J. Chem. Phys.* (2001)
- [9] Persson. *Phys. Rev. Lett.* (2001)
- [10] Persson, Bucher, Chiaia. *Phys. Rev. B* (2002)
- [11] Müser. *Phys. Rev. Lett.* (2008)

Cross-link studies

- [12] Manners, Greenwood. *Wear* (2006)
- [13] Carbone, Bottiglione. *J. Mech. Phys. Solids* (2008)
- [14] Paggi, Ciavarella. *Wear* (2010)

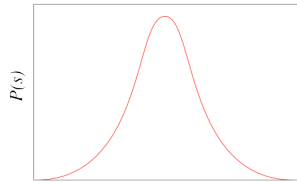
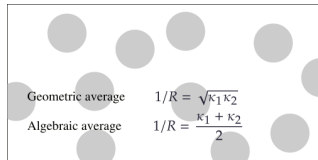


Fig. Asperity based models

Analytical models

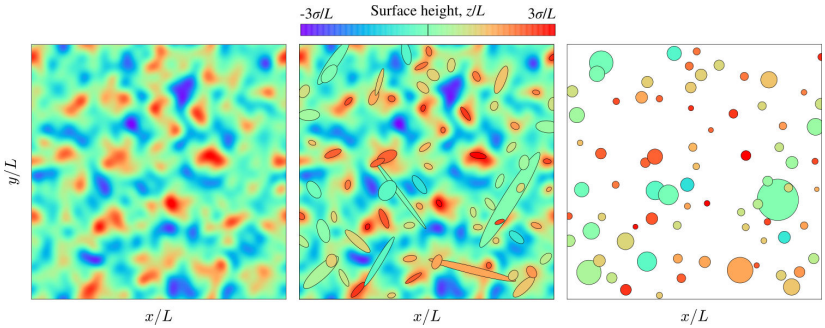


Fig. Roughness and detected asperities for $L/\lambda_l = 4$ and $L/\lambda_s = 16$

Analytical models

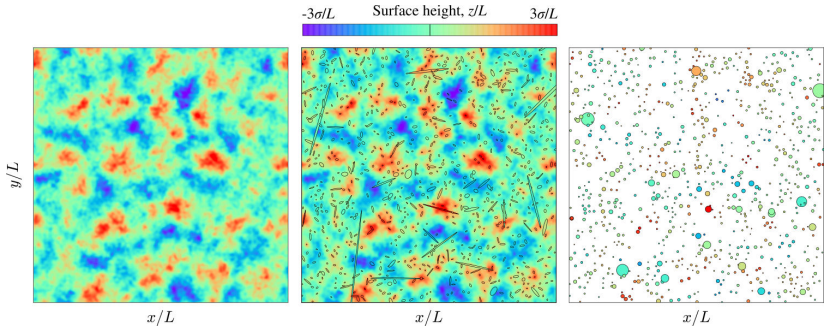


Fig. Roughness and detected asperities for $L/\lambda_l = 4$ and $L/\lambda_s = 64$

Analytical models

$$\text{contact radius: } a = \left(\frac{3RF}{4E^*} \right)^{1/3} \quad \text{contact force: } F = \frac{4}{3} R^{1/2} E^* \delta^{3/2}$$

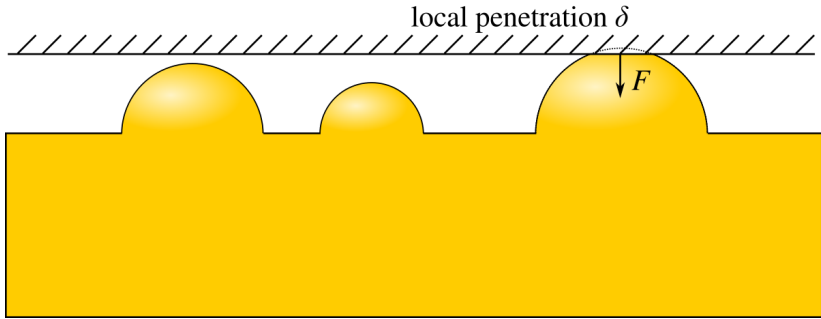


Fig. Hertz's theory of contact

Analytical models

Asperity based models

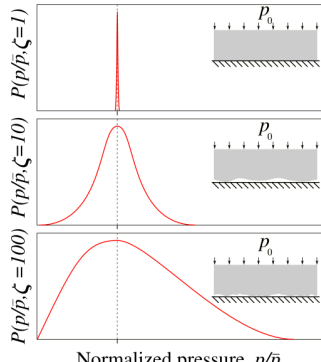
- [1] Greenwood, Williamson. *P Roy Soc Lond A Mat* (1966)
- [2] Bush, Gibson, Thomas. *Wear* (1975)
- [3] Mc Cool. *Wear* (1986)
- [4] Thomas. *Rough Surfaces* (1999)
- [5] Greenwood. *Wear* (2006)
- [6] Carbone. *J. Mech. Phys. Solids* (2009)
- [7] Ciavarella, Greenwood, Paggi. *Wear* (2008)

Persson's model

- [8] Persson. *J. Chem. Phys.* (2001)
- [9] Persson. *Phys. Rev. Lett.* (2001)
- [10] Persson, Bucher, Chiaia. *Phys. Rev. B* (2002)
- [11] Müser. *Phys. Rev. Lett.* (2008)

Cross-link studies

- [12] Manners, Greenwood. *Wear* (2006)
- [13] Carbone, Bottiglione. *J. Mech. Phys. Solids* (2008)
- [14] Paggi, Ciavarella. *Wear* (2010)



Normalized pressure, p/\bar{p}

Fig. Persson's model

$$\frac{\partial P(p, \zeta)}{\partial V(\zeta)} = \frac{1}{2} \frac{\partial^2 P(p, \zeta)}{\partial p^2} \quad P(0, \zeta) = 0$$

$$V(\zeta) = \frac{1}{2} E^* m_2(\zeta) = \frac{\pi E^*}{2} \int \frac{\zeta k_l}{k_l} k^3 \Phi^p(k) dk$$

Comparison of models

Asperity based models

1. Evolution of the real contact area $A(p_0)$ for $A/A_0 \rightarrow 0$

$$\frac{A}{A_0} = \frac{\kappa}{\sqrt{\langle |\nabla z|^2 \rangle}} \frac{p_0}{E^*}$$

$\kappa_{\text{BGT}} = \sqrt{2\pi} \approx 2.5$ according to [2-5]

$\kappa_P = \sqrt{8/\pi} \approx 1.6$ according to [6-7]

2. Evolution of the real contact area $A(p_0)$ for $\forall A/A_0$

$\frac{A}{A_0} = A(p_0, \alpha)/A_0$ according to [2-5]

$\frac{A}{A_0} = \operatorname{erf}\left(\sqrt{\frac{2}{\langle |\nabla z|^2 \rangle}} \frac{p_0}{E^*}\right)$ according to [6-7]

[1] Greenwood, Williamson, P Roy Soc Lond A Mat 295 (1966)

[2] Bush, Gibson, Thomas, Wear 35 (1975)

[3] McCool, Wear 107 (1986)

[4] Thomas, Rough Surfaces (1999)

[5] Greenwood, Wear 261 (2006)

[6] Persson, J. Chem. Phys. 115 (2001)

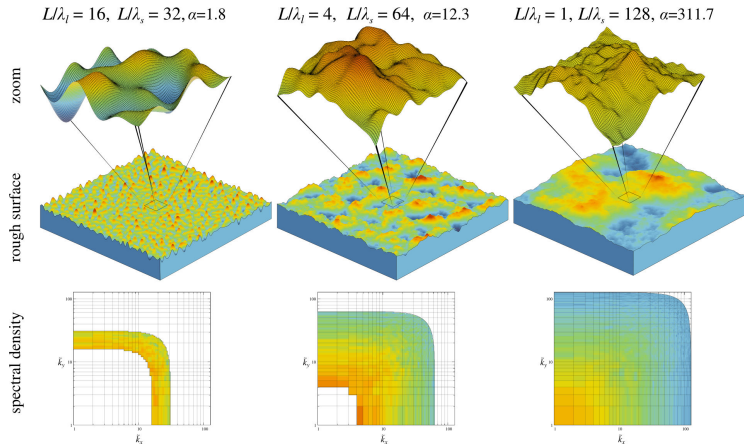
[7] Persson, Phys. Rev. Lett. 87 (2001)

[8] Persson, Bucher, Chiaia, Phys. Rev. B 65 (2002)

[9] Muser, Phys. Rev. Lett. 100, (2008)

Simulations set-up

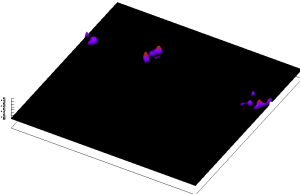
- Cut-off parameters: $L/\lambda_l \otimes L/\lambda_s = \{1, 2, 4, 8, 16\} \otimes \{32, 64, 128, 256, 512\}$
- Hurst exponent $H = \{0.4, 0.8\}$
- 10 random surface realizations per combination of parameters
- Discretization: $\{L/\Delta x\} \times \{L/\Delta x\} = 2048 \times 2048$
- Search for contact area A' , gap field $g(x, y)$ and gap PDF $P(g)$



Contact area and contact pressure evolution

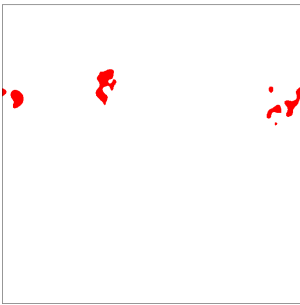
$k_l=1, k_s=32, H=0.8$

Contact pressure, $p(x,y)$



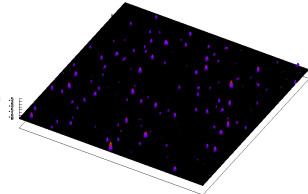
$k_l=1, k_s=32, H=0.8$

Contact area, $a(x,y)$



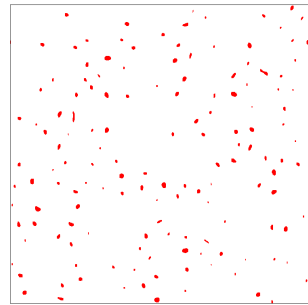
$k_l=16, k_s=32, H=0.8$

Contact pressure, $p(x,y)$

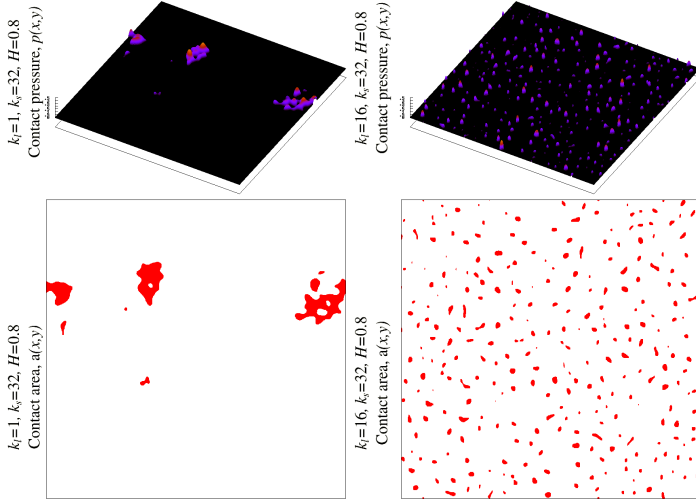


$k_l=16, k_s=32, H=0.8$

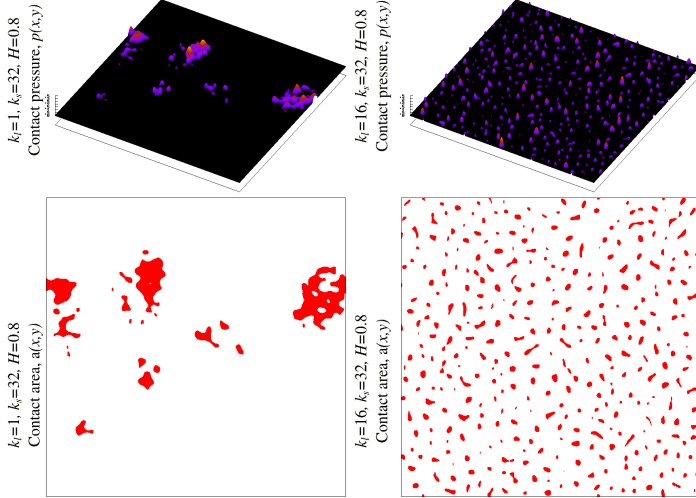
Contact area, $a(x,y)$



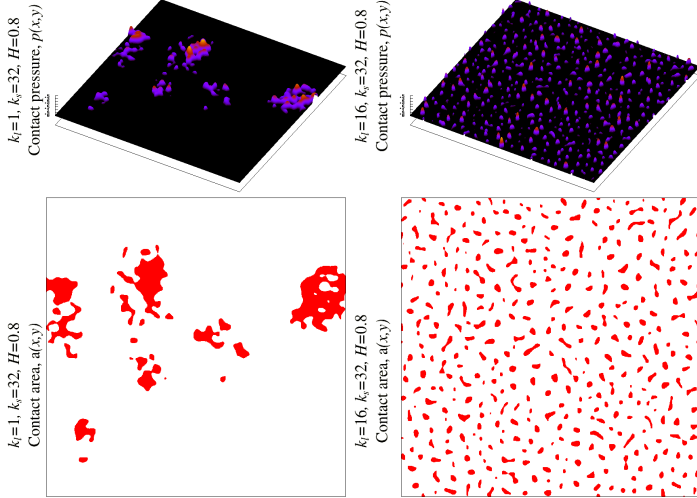
Contact area and contact pressure evolution



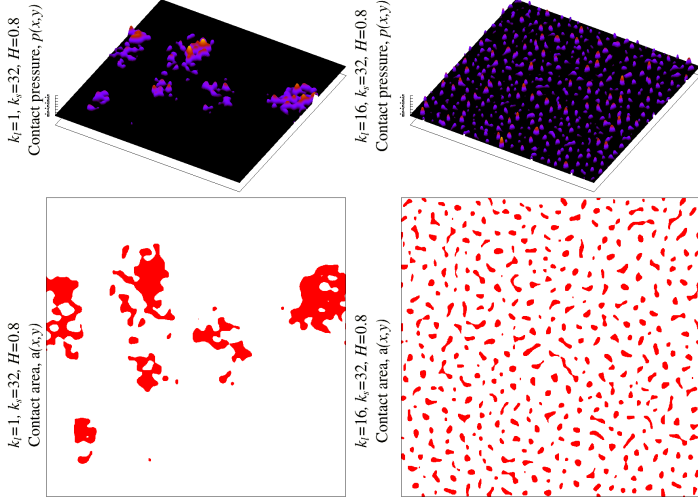
Contact area and contact pressure evolution



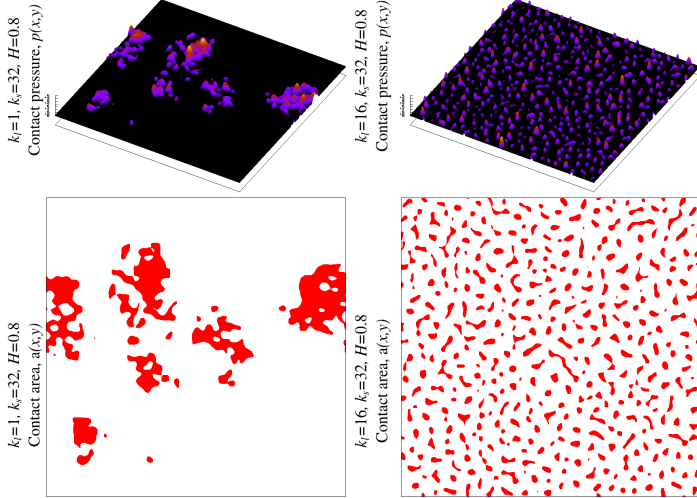
Contact area and contact pressure evolution



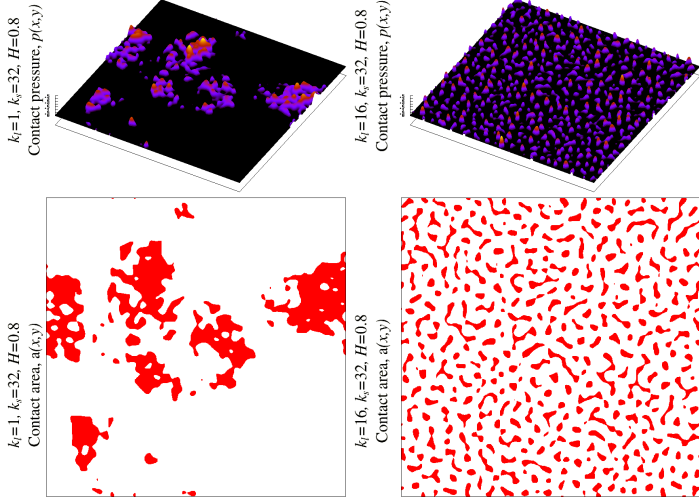
Contact area and contact pressure evolution



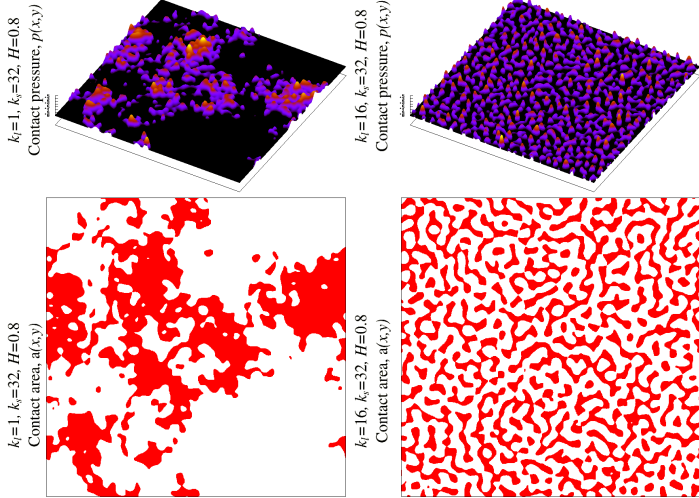
Contact area and contact pressure evolution



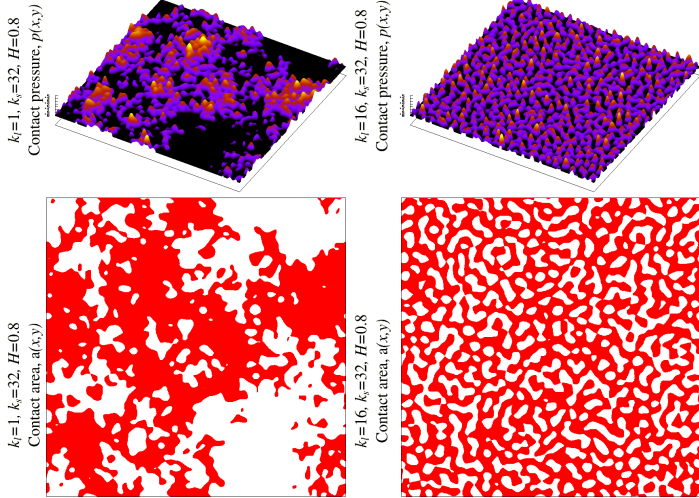
Contact area and contact pressure evolution



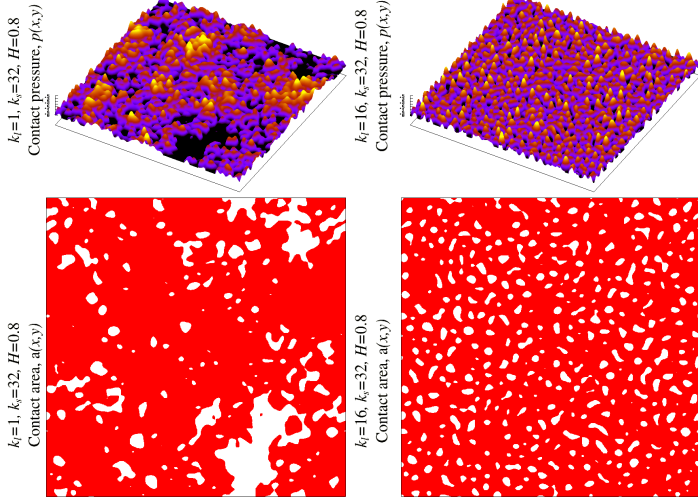
Contact area and contact pressure evolution



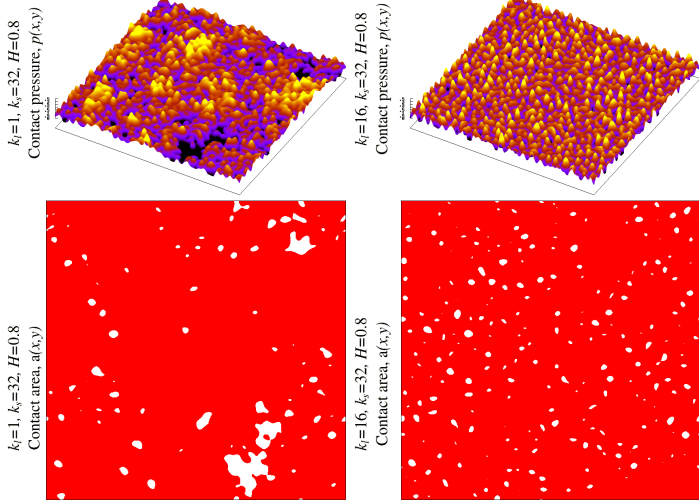
Contact area and contact pressure evolution



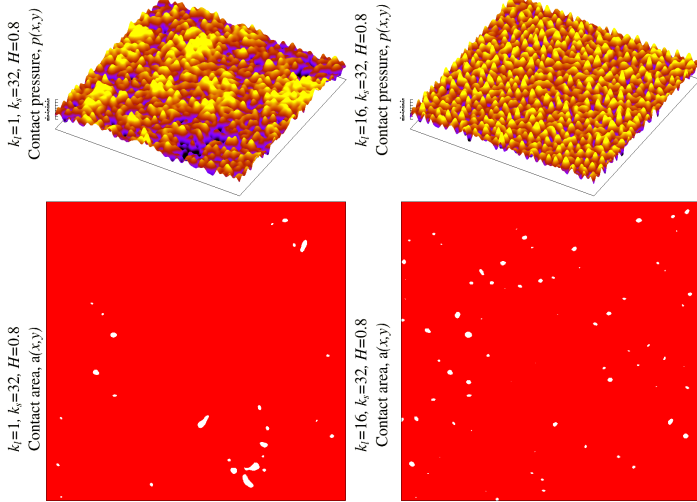
Contact area and contact pressure evolution



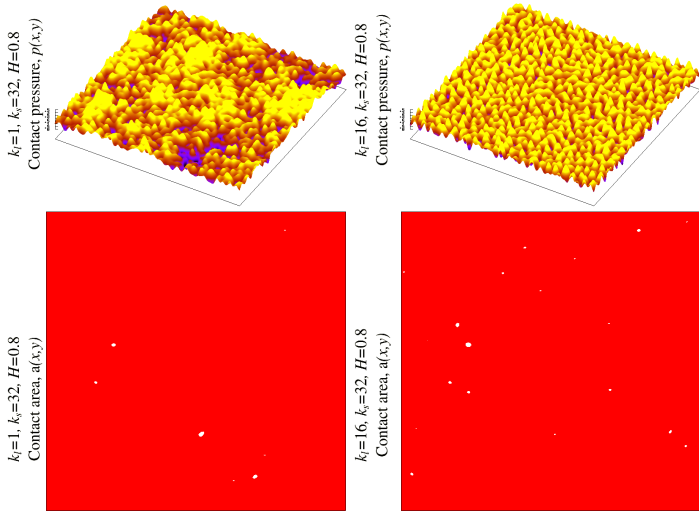
Contact area and contact pressure evolution



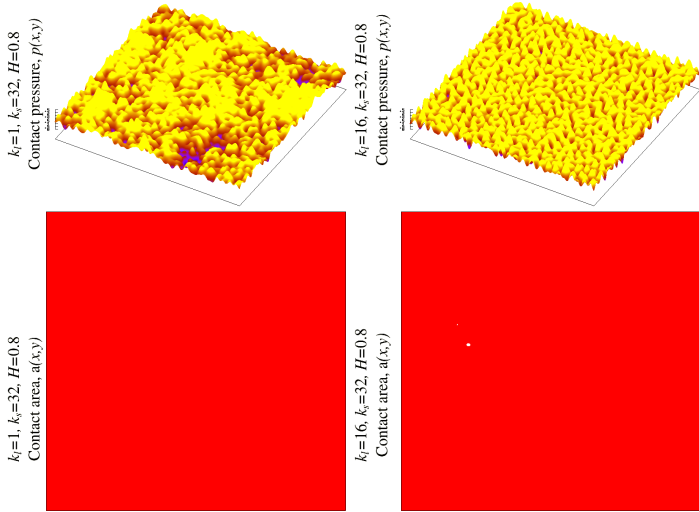
Contact area and contact pressure evolution



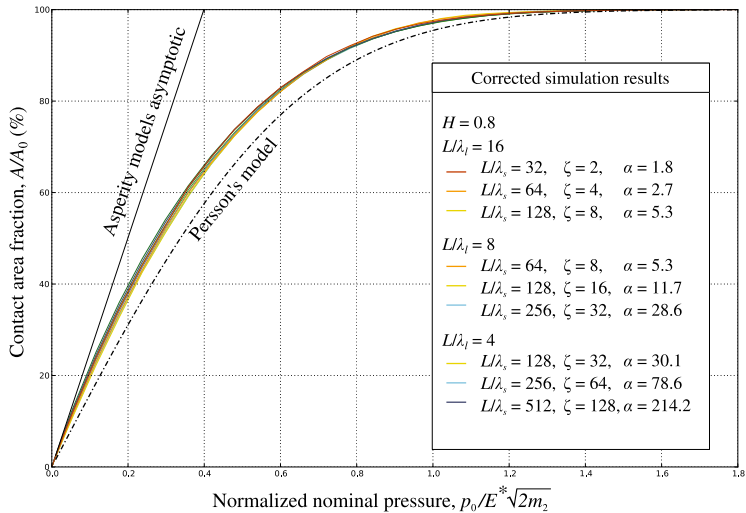
Contact area and contact pressure evolution



Contact area and contact pressure evolution



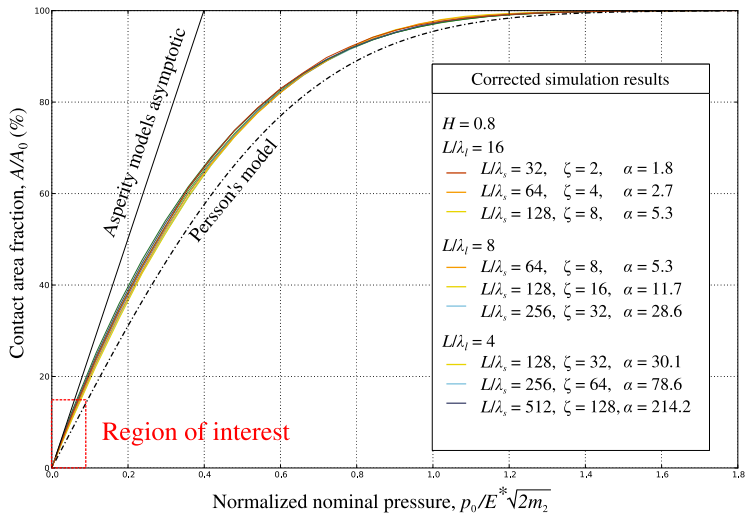
Results: contact area



Multi-asperity models asymptotic^[1,2], Persson's model^[3]

[1] Bush, Gibson, Thomas, Wear 35 (1975), [2] Carbone, Bottiglione. J. Mech. Phys. Solids (2008), [3] Persson. J. Chem. Phys. (2001)

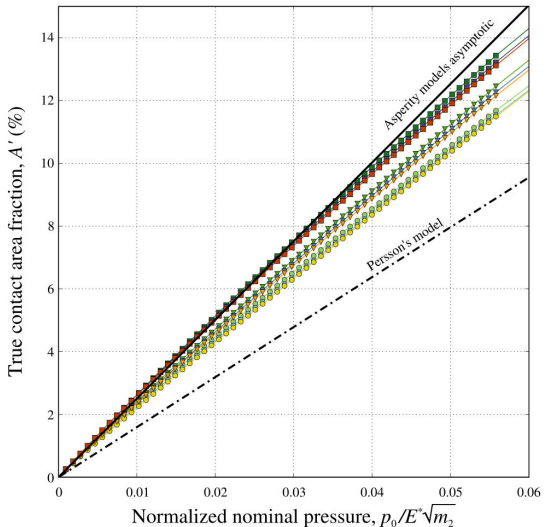
Results: contact area



Multi-asperity models asymptotic^[1,2], Persson's model^[3]

[1] Bush, Gibson, Thomas, Wear 35 (1975), [2] Carbone, Bottiglione. J. Mech. Phys. Solids (2008), [3] Persson. J. Chem. Phys. (2001)

Real contact area: interpretation of results?



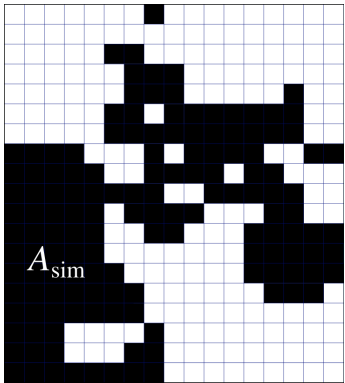
Raw data

[1] Yastrebov, Anciaux, Molinari, Int J Solids Struct 52 (2015)

Numerical error correction

- Contact area is overestimated in simulations:

$$A_{\text{sim}} > A_*$$



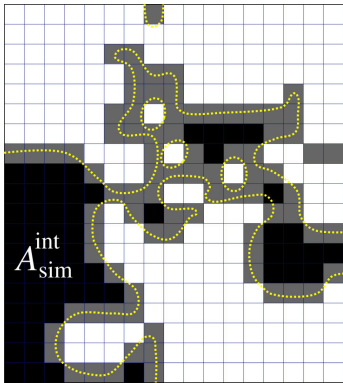
Numerical error correction

- Contact area is overestimated in simulations:

$$A_{\text{sim}} > A_*$$

- The overestimation is localized at boundary nodes:

$$A_{\text{sim}} > A_* > A_{\text{sim}}^{\text{int}}$$



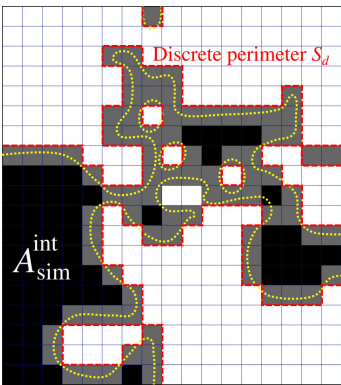
Numerical error correction

- Contact area is overestimated in simulations:
 $A_{\text{sim}} > A_*$
- The overestimation is localized at boundary nodes:

$$A_{\text{sim}} > A_* > A_{\text{sim}}^{\text{int}}$$

- Boundary area \sim perimeter S_d :

$$A_{\text{sim}} - A_{\text{sim}}^{\text{int}} = S_d \Delta x$$



Numerical error correction

- Contact area is overestimated in simulations:

$$A_{\text{sim}} > A_*$$

- The overestimation is localized at boundary nodes:

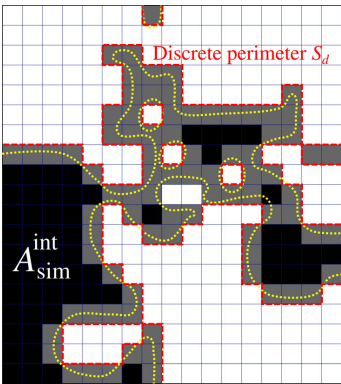
$$A_{\text{sim}} > A_* > A_{\text{sim}}^{\text{int}}$$

- Boundary area \sim perimeter S_d :

$$A_{\text{sim}} - A_{\text{sim}}^{\text{int}} = S_d \Delta x$$

- Manhattan S_d vs Euclidean metric S :

$$\langle S \rangle = \frac{\pi}{4} \langle S_d \rangle$$



Numerical error correction

- Contact area is overestimated in simulations:

$$A_{\text{sim}} > A_*$$

- The overestimation is localized at boundary nodes:

$$A_{\text{sim}} > A_* > A_{\text{sim}}^{\text{int}}$$

- Boundary area \sim perimeter S_d :

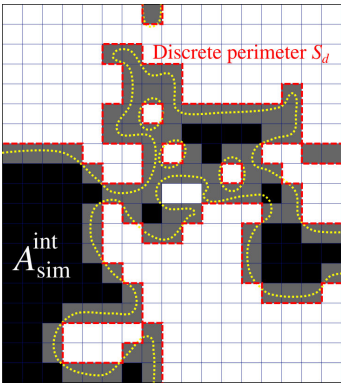
$$A_{\text{sim}} - A_{\text{sim}}^{\text{int}} = S_d \Delta x$$

- Manhattan S_d vs Euclidean metric S :

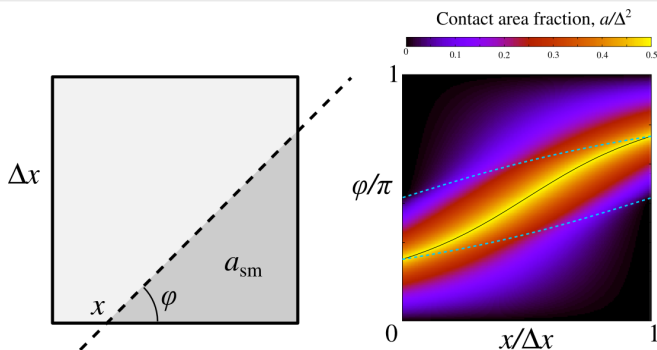
$$\langle S \rangle = \frac{\pi}{4} \langle S_d \rangle$$

- True contact area estimation:

$$A_* \approx A_{\text{sim}} - \beta \frac{\pi}{4} S_d \Delta x$$



Numerical error correction: corrective factor



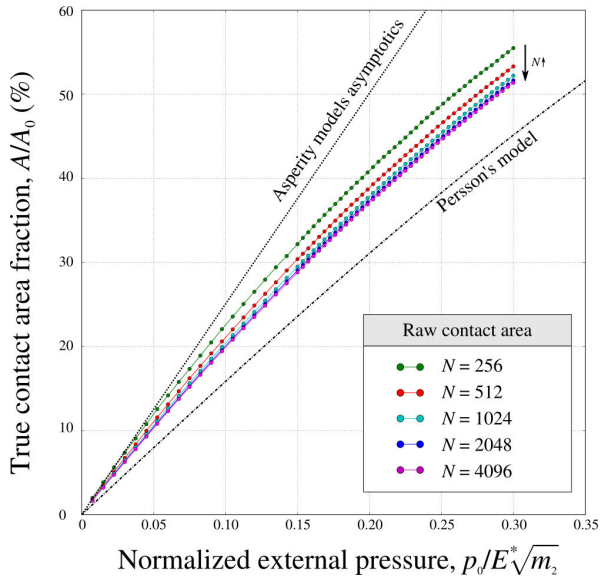
Corrective factor $\beta = \frac{\langle a_{\text{sm}} \rangle}{\Delta x^2} = \frac{1}{\Delta x^2} \int_0^h \int_0^\pi a_{\text{sm}} P(x, \phi) dx d\phi = \frac{\pi - 1 + \ln 2}{6\pi}$

$$\beta = 0.150387618994810151606955\dots$$

True area estimation:

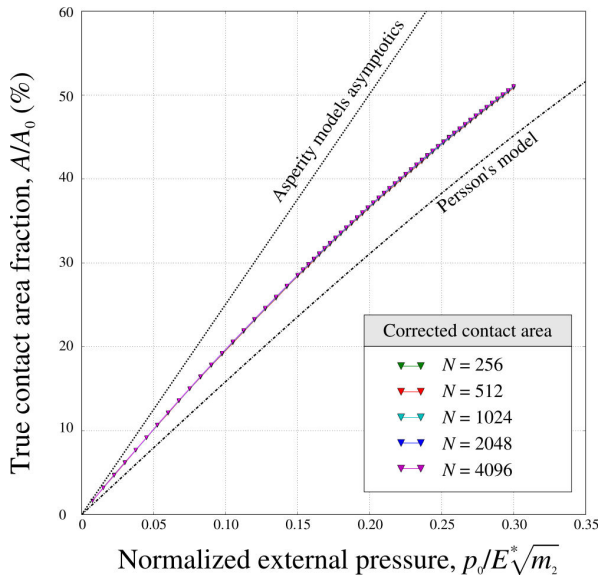
$$A_* \approx A_{\text{sim}} - \frac{\pi - 1 + \ln 2}{24} S_d \Delta x$$

Numerical error correction: convergence study



[1] Yastrebov, Anciaux, Molinari, Tribol Int 114 (2017)

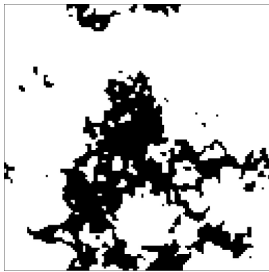
Numerical error correction: convergence study



[1] Yastrebov, Anciaux, Molinari, Tribol Int 114 (2017)

Morphological correction

- Morphology of contact clusters



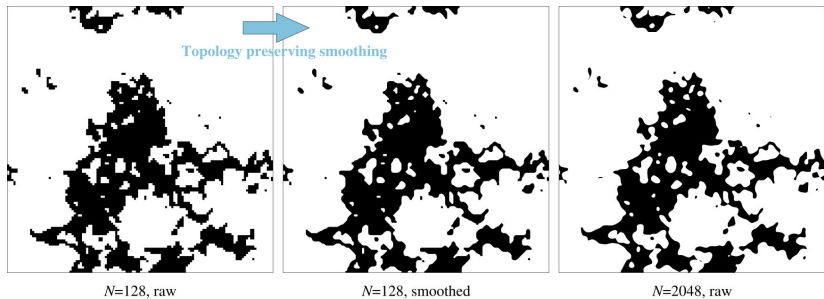
$N=128$, raw



$N=2048$, raw

Morphological correction

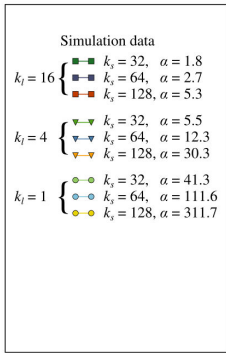
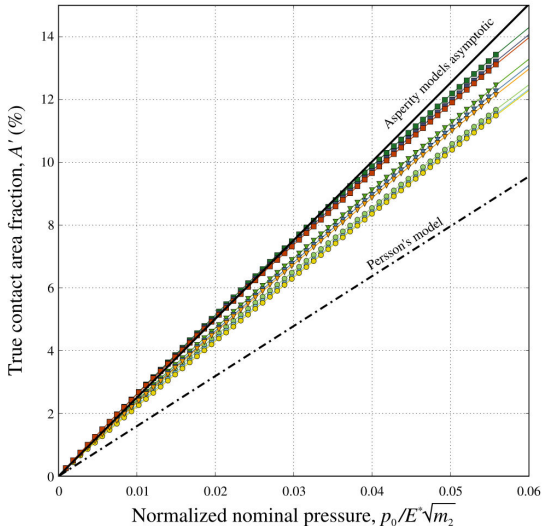
- Morphology of contact clusters



Topologically preserving smoothing results in realistic cluster geometry

[1] Couplie & Bertrand, *J Electr Imag* 13 (2004)

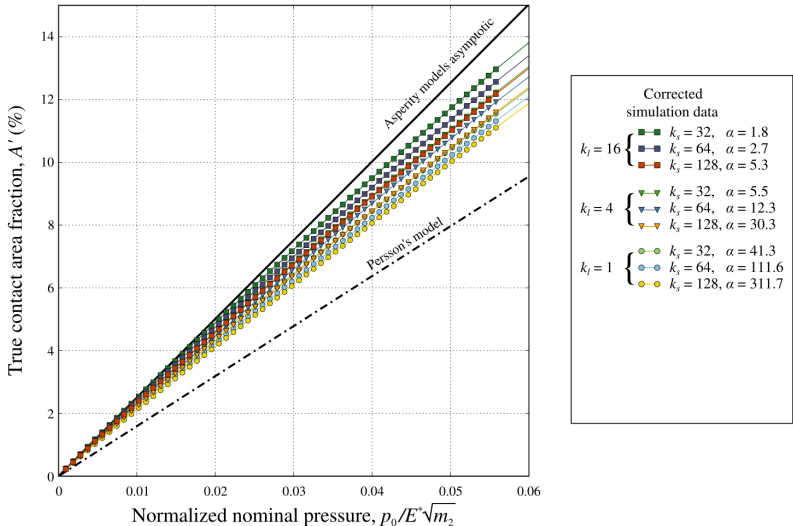
Real contact area: accurate results



Raw data

[1] Yastrebov, Anciaux, Molinari, Int J Solids Struct 52 (2015)

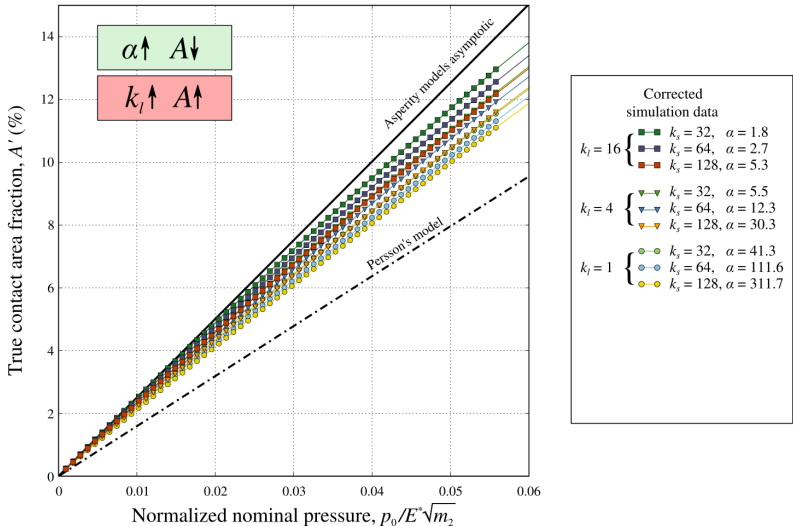
Real contact area: accurate results



Corrected data

[2] Yastrebov, Anciaux, Molinari, *J Mech Phys Solids* 107 (2017)

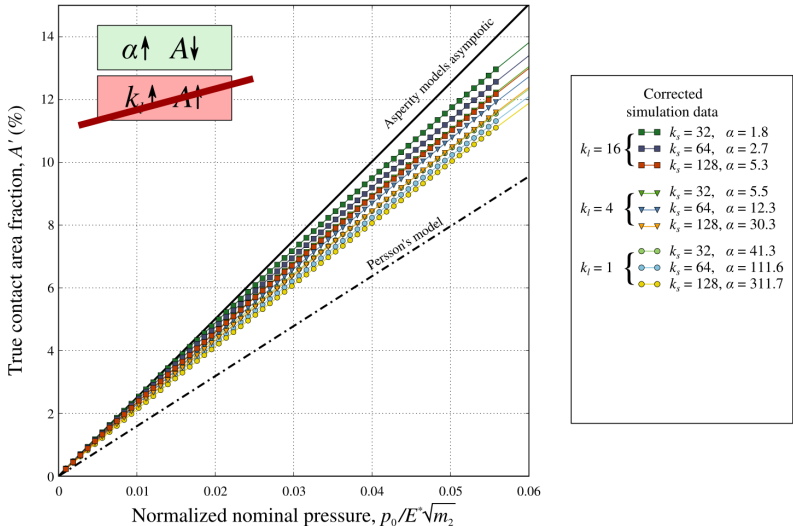
Real contact area: accurate results



Corrected data

[2] Yastrebov, Anciaux, Molinari, *J Mech Phys Solids* 107 (2017)

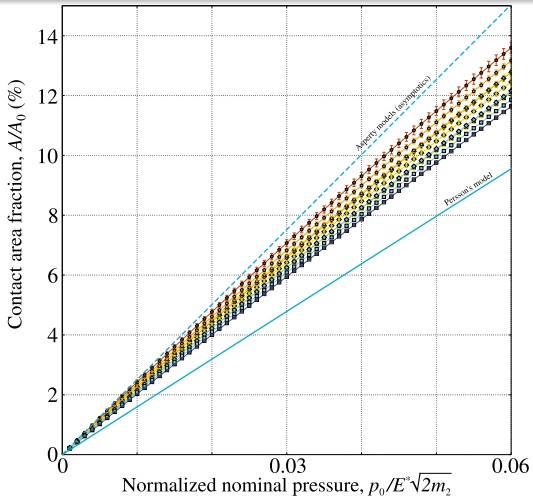
Real contact area: accurate results



Corrected data

[2] Yastrebov, Anciaux, Molinari, *J Mech Phys Solids* 107 (2017)

Results: contact area



Corrected simulation results

$$H = 0.8$$

$$L/\lambda_l = 16$$

- $L/\lambda_s = 32, \zeta = 2, \alpha = 1.8$
- $L/\lambda_s = 64, \zeta = 4, \alpha = 2.7$
- $L/\lambda_s = 128, \zeta = 8, \alpha = 5.3$

$$L/\lambda_l = 8$$

- $L/\lambda_s = 64, \zeta = 8, \alpha = 5.3$
- $L/\lambda_s = 128, \zeta = 16, \alpha = 11.7$
- $L/\lambda_s = 256, \zeta = 32, \alpha = 28.6$

$$L/\lambda_l = 4$$

- $L/\lambda_s = 128, \zeta = 32, \alpha = 30.1$
- $L/\lambda_s = 256, \zeta = 64, \alpha = 78.6$
- $L/\lambda_s = 512, \zeta = 128, \alpha = 214.2$

Corrected contact area (discretization independent): "magic" formula^[1,2]

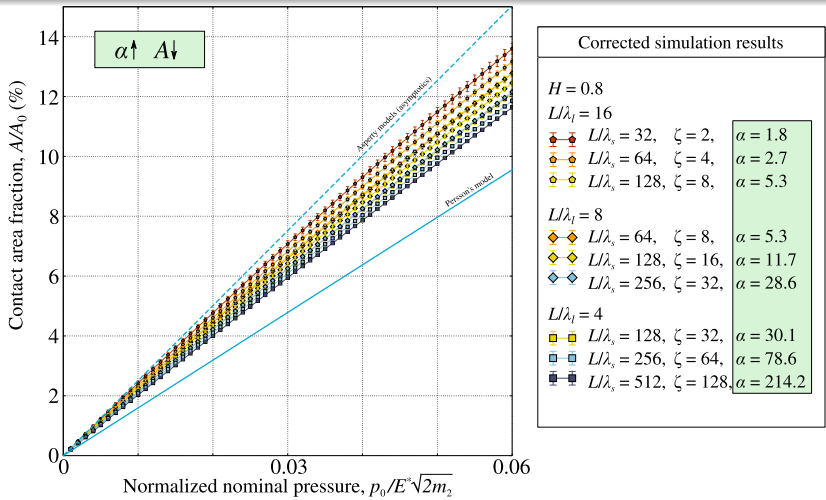
$$A_* \approx A_{\text{sim}} - \frac{\pi - 1 + \ln 2}{24} S_d \Delta x,$$

where S_d is the integral perimeter of the contact zones.

[1] Yastrebov, Anciaux, Molinari, *Tribol. Int.* 114 (2017)

[2] Yastrebov, Anciaux, Molinari, *J Mech Phys Solids* 107 (2017)

Results: contact area



Corrected contact area (discretization independent): “magic” formula^[1,2]

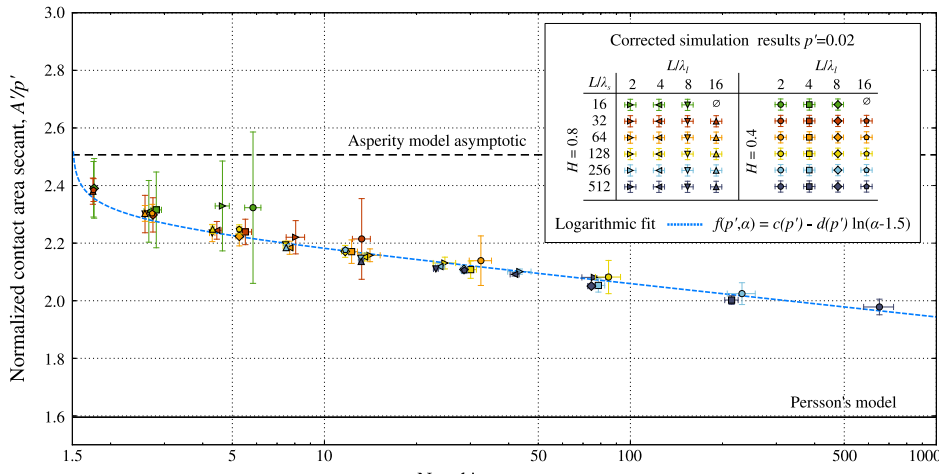
$$A_* \approx A_{\text{sim}} - \frac{\pi - 1 + \ln 2}{24} S_d \Delta x,$$

where S_d is the integral perimeter of the contact zones.

[1] Yastrebov, Anciaux, Molinari, *Tribol. Int.* 114 (2017)

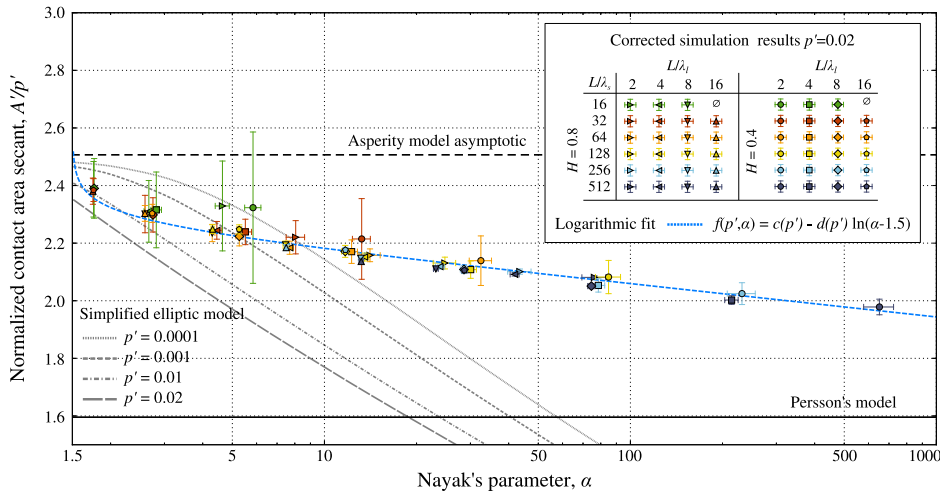
[2] Yastrebov, Anciaux, Molinari, *J Mech Phys Solids* 107 (2017)

Role of Nayak parameter α



Numerical results: [1] Yastrebov, Anciaux, Molinari, J Mech Phys Solids 107 (2017)

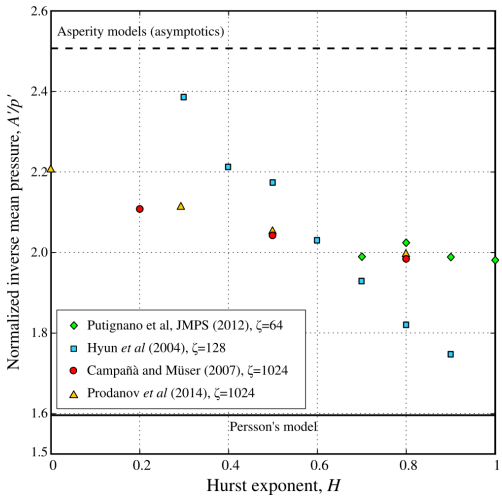
Role of Nayak parameter α



Numerical results: [1] Yastrebov, Anciaux, Molinari, J Mech Phys Solids 107 (2017)

Simplified elliptic model: [2] Greenwood, Wear (2006)

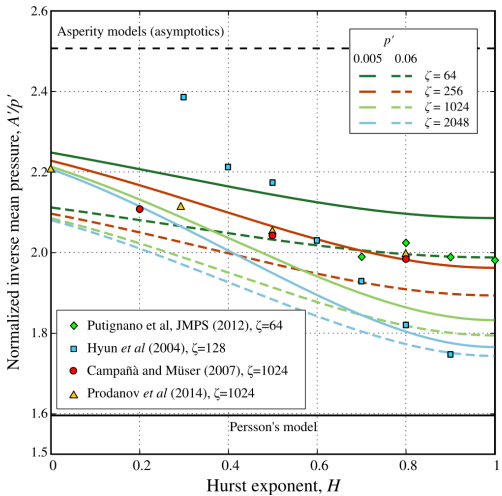
Role of Nayak parameter α



Comparison with other numerical studies
Nayak-Hurst relationship

$$\alpha(H, \zeta) = \frac{3}{2} \frac{(1-H)^2}{H(H-2)} \frac{(\zeta^{-2H}-1)(\zeta^{4-2H}-1)}{(\zeta^{2-2H}-1)^2}$$

Role of Nayak parameter α



Comparison with other numerical studies
Nayak-Hurst relationship

$$\alpha(H, \zeta) = \frac{3}{2} \frac{(1-H)^2}{H(H-2)} \frac{(\zeta^{-2H}-1)(\zeta^{4-2H}-1)}{(\zeta^{2-2H}-1)^2}$$

Phenomenological relationship

- Contact area A grows with applied pressure p_0 as

$$\frac{A}{A_0} = a(\alpha) \frac{p_0}{E^* \sqrt{2m_2}} - b(\alpha) \left[\frac{p_0}{E^* \sqrt{2m_2}} \right]^2$$

- Contact area fraction $A' = A/A_0$ grows with normalized applied pressure $p' = p_0/E^* \sqrt{2m_2}$

$$A' = a(\alpha)p' - b(\alpha)p'^2$$

- With \approx universal adimensional constants:

$$a(\alpha) = 2.35 - 0.057 \ln(\alpha - 1.5)$$

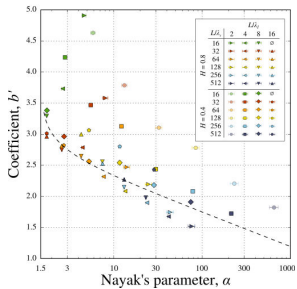
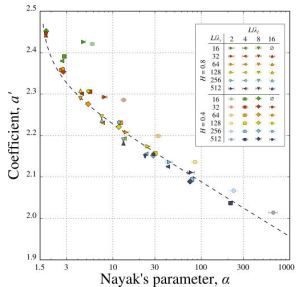
$$b(\alpha) = 2.85 - 0.24 \ln(\alpha - 1.5)$$

- Pressure dependent friction coefficient:

$$\mu(p') = \mu_0 \left[1 - \frac{b(\alpha)}{a(\alpha)} p' \right]$$

with $\mu_0 = a(\alpha)\tau_{\max}/E^* \sqrt{2m_2}$,

τ_{\max} is the maximum shear traction the contact interface can bear.



Conclusions

- Contact area growth almost linearly for small pressures and saturates at bigger pressure
- The key parameter of the contact area growth is the RMS slope or its variance $2m_2$
- Contact area depends weakly on Nayak parameter $\alpha = m_0 m_4 / m_2^2$

$$A' = a(\alpha)p' - b(\alpha)p'^2$$

with $a(\alpha) = 2.35 - 0.057 \ln(\alpha - 1.5)$, $b(\alpha) = 2.85 - 0.24 \ln(\alpha - 1.5)$

- No effect of fractal dimension D_f *per se* on the contact area
it affects the contact area only through the Nayak parameter

Flow through the
contact interface

Problem statement

Problem

- Thin creeping flow in contact interface:
Navier-Stokes → Stokes → Reynolds equation
- In addition: incompressible fluid, immobile walls:

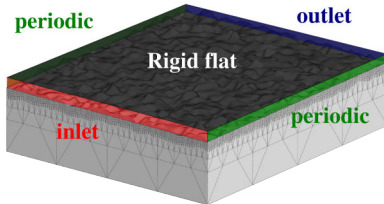
$$\nabla \cdot \underline{q} = 0, \quad \underline{q} = -\frac{g^3}{12\mu} \nabla p_f$$

$\underline{q}(x, y)$ is the fluid flux,

$\underline{g}(x, y)$ is the gap (opening) fields,

$p_f(x, y)$ hydrostatic fluid pressure,

μ is the dynamic viscosity.



- Gap profile $g(x, y)$ for $x, y \in (0, L)$
- At inlet: $p_f = p_{in}$
- At outlet: $p_f = p_{out}$
- At lateral sides: periodic
 $q_n(y = L) = -q_n(y = 0)$
- Linear problem: use FEM

Analytical approach

Effective flow estimation

- Averaging over surface $\langle x \rangle = 1/A_0 \int_{A_0} x \, dA$ gives:

$$\langle \underline{q} \rangle = -\underline{\underline{K}}_{\text{eff}} \cdot \langle \nabla p_f \rangle$$

- For isotropic case, normalized scalar **effective transmissivity** along pressure drop OX :

$$K'_{\text{eff}} = -\frac{12\mu \langle q_x \rangle L}{m_0^{3/2} (p_{\text{in}} - p_{\text{out}})}$$

- Using effective medium^[1,2] approach

$$(1 - A') \int_0^\infty \frac{g^3 P(g)}{g^3 + K'_{\text{eff}} m_0^{3/2}} dg = \frac{1}{2}$$

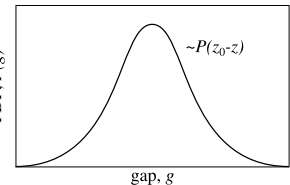
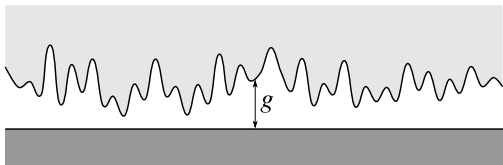
$A' = A/A_0$ is the contact area fraction, $P(g)$ is the gap probability density.

[1] Kirkpatrick. Rev Modern Phys, 45 (1973)

[2] Lorenz & Persson. Europ Phys J E: Soft Matter, 31 (2010)

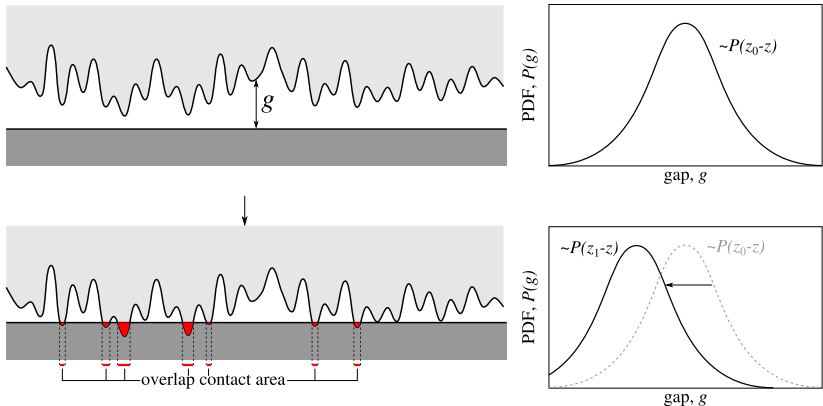
Danger: geometrical overlap

- Geometrical overlap model is highly inaccurate

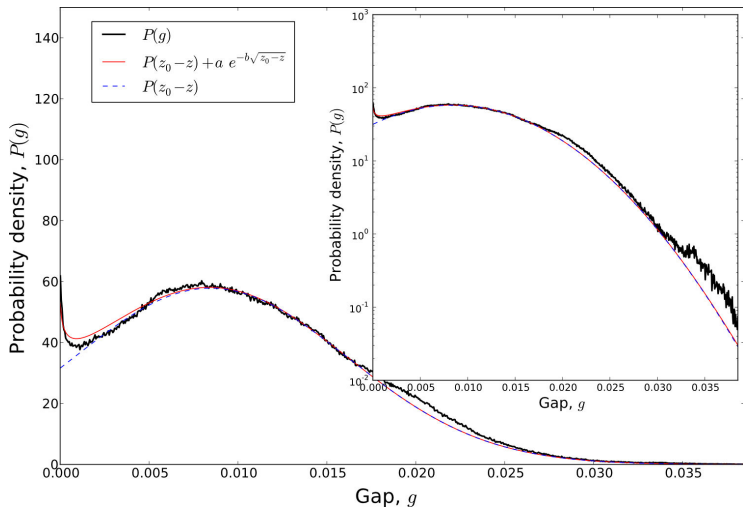


Danger: geometrical overlap

- Geometrical overlap model is highly inaccurate

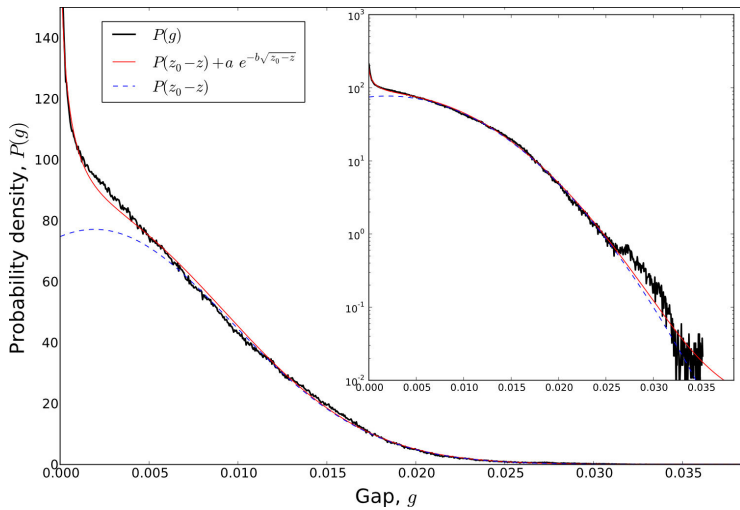


Solid contact results: gap distribution



Gap probability density VS geometrical overlap model (dashed line)
Near contact interface $P(g) \sim P(z_0 - z) + a \exp(-b \sqrt{z_0 - z})$

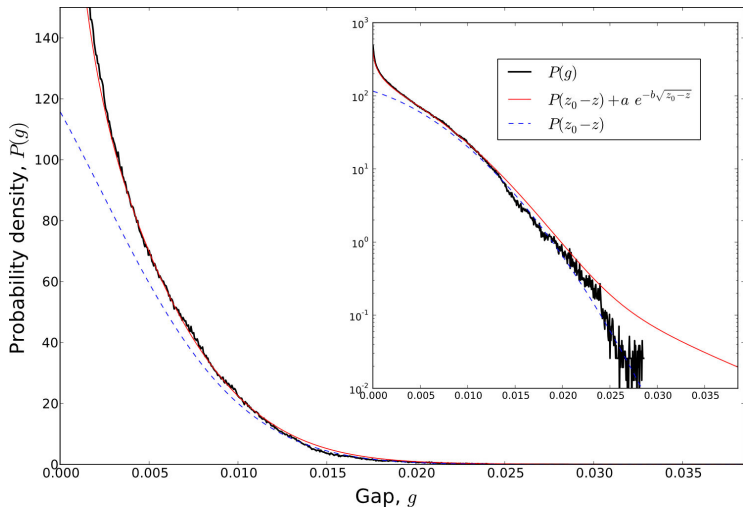
Solid contact results: gap distribution



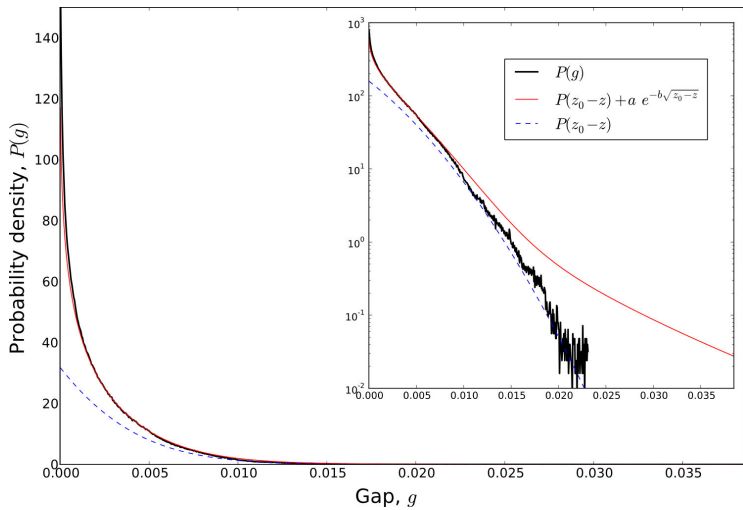
Area fraction $A' = 9.5\%$

Gap probability density VS geometrical overlap model (dashed line)
Near contact interface $P(g) \sim P(z_0 - z) + a \exp(-b \sqrt{z_0 - z})$

Solid contact results: gap distribution

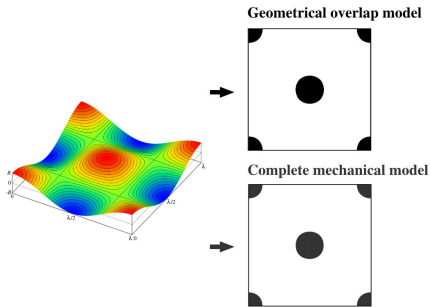


Solid contact results: gap distribution



Geometrical overlap: morphology and percolation

- Geometrical overlap model is highly inaccurate^[1,2]

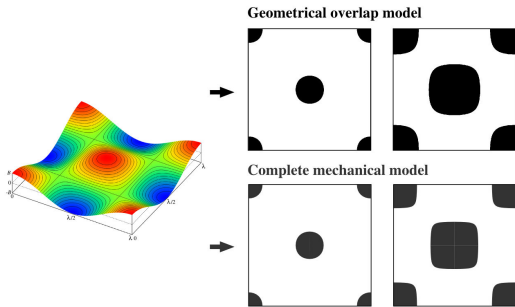


[1] Dapp, Lücke, Persson, Müser, *Phys. Rev. Lett.* 108 (2012)

[2] Yastrebov, Anciaux, Molinari. *Tribol Lett*, 56 (2014)

Geometrical overlap: morphology and percolation

- Geometrical overlap model is highly inaccurate^[1,2]

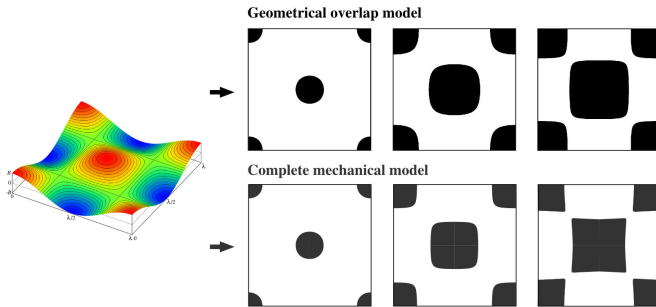


[1] Dapp, Lücke, Persson, Müser, *Phys. Rev. Lett.* 108 (2012)

[2] Yastrebov, Anciaux, Molinari. *Tribol Lett*, 56 (2014)

Geometrical overlap: morphology and percolation

- Geometrical overlap model is highly inaccurate^[1,2]

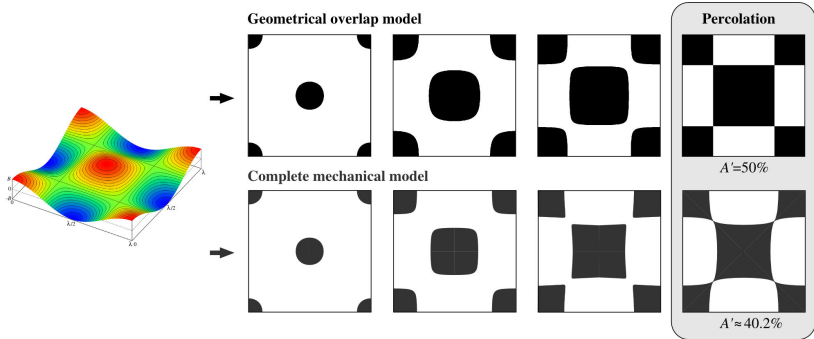


[1] Dapp, Lücke, Persson, Müser, *Phys. Rev. Lett.* 108 (2012)

[2] Yastrebov, Anciaux, Molinari. *Tribol Lett*, 56 (2014)

Geometrical overlap: morphology and percolation

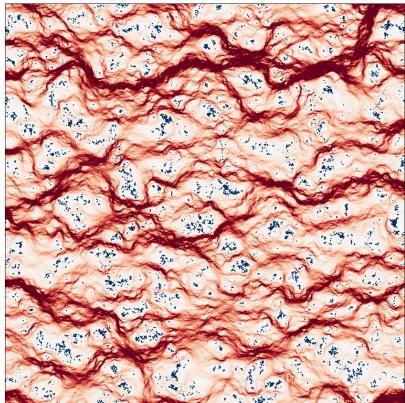
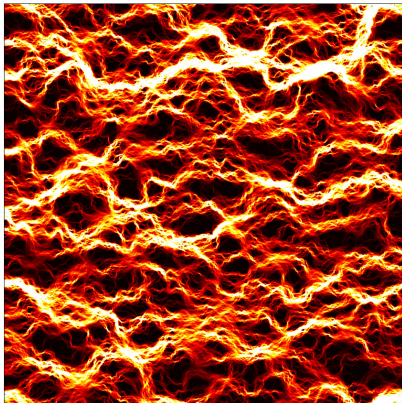
- Geometrical overlap model is highly inaccurate^[1,2]



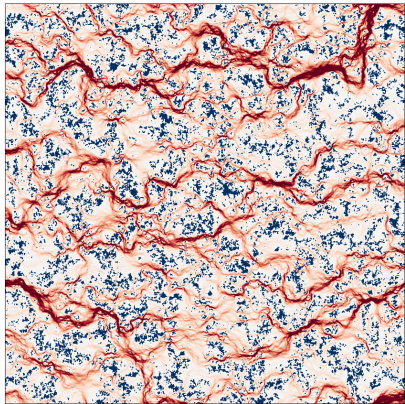
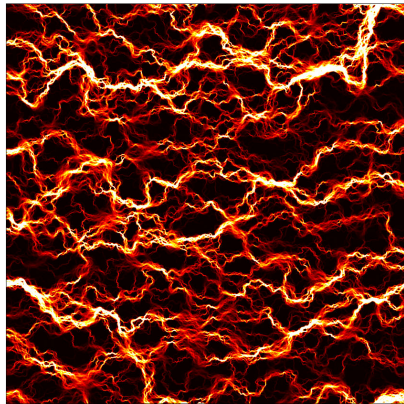
[1] Dapp, Lücke, Persson, Müser, *Phys. Rev. Lett.* 108 (2012)

[2] Yastrebov, Anciaux, Molinari. *Tribol Lett*, 56 (2014)

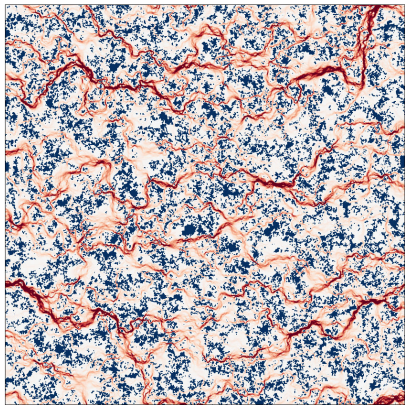
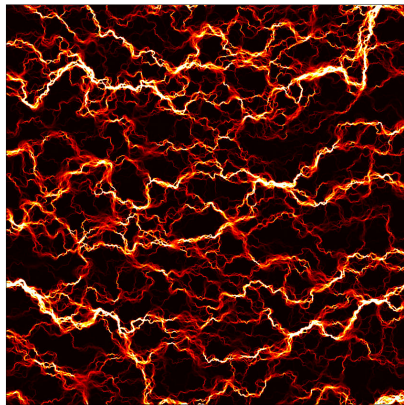
Creeping fluid transport



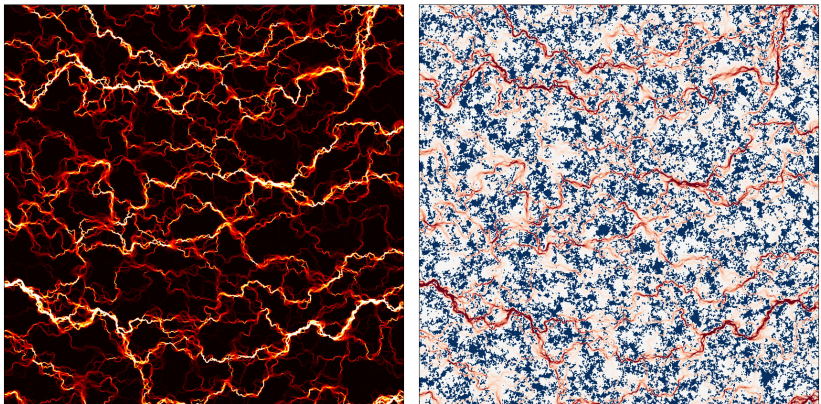
Creeping fluid transport



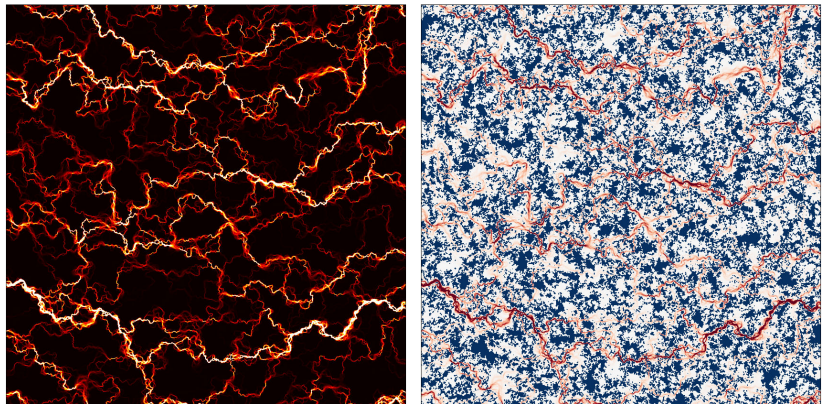
Creeping fluid transport



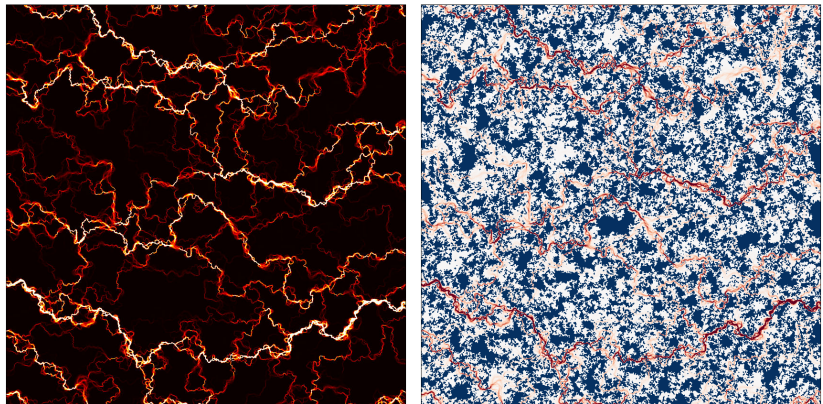
Creeping fluid transport



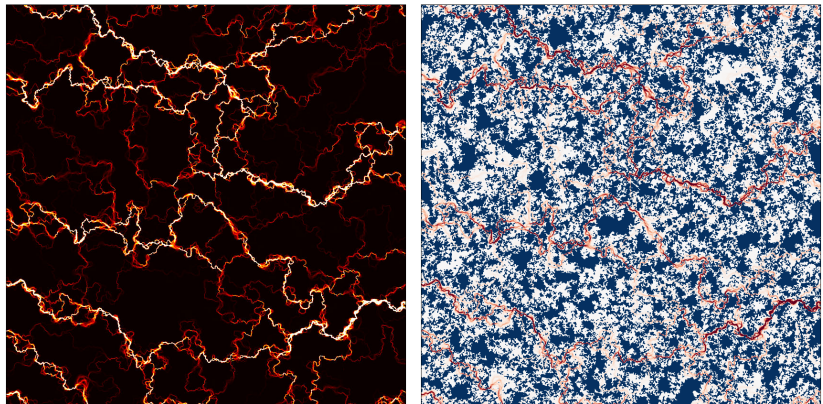
Creeping fluid transport



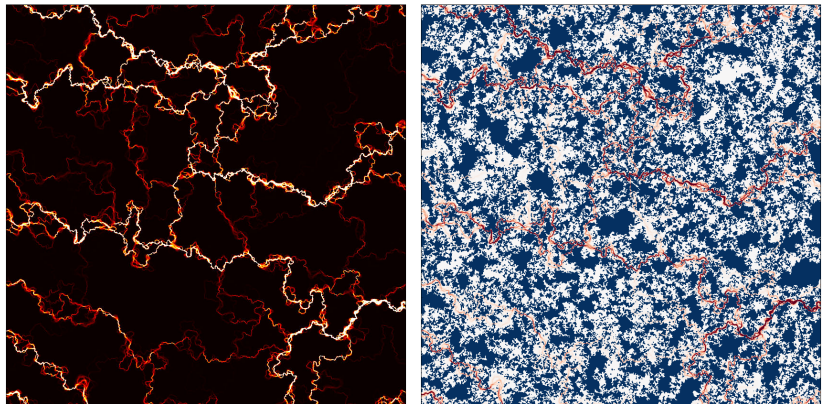
Creeping fluid transport



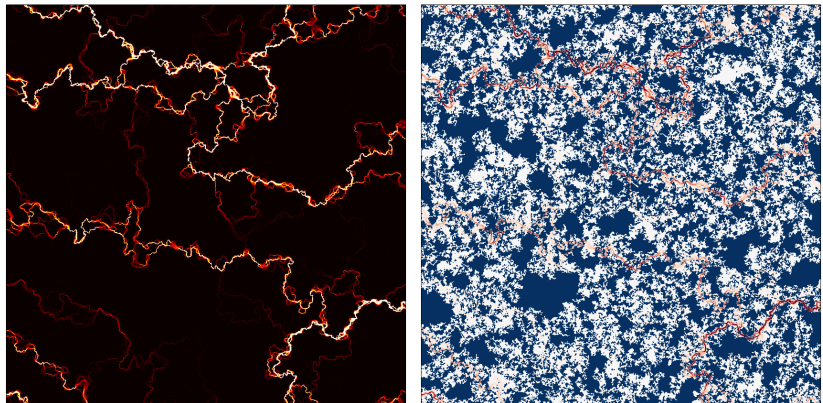
Creeping fluid transport



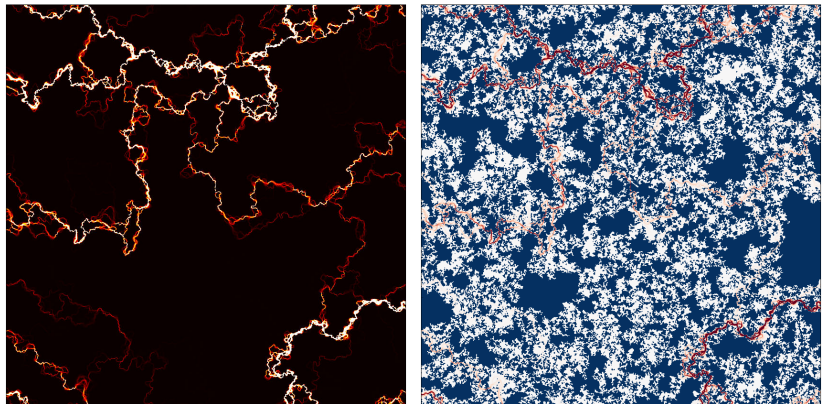
Creeping fluid transport



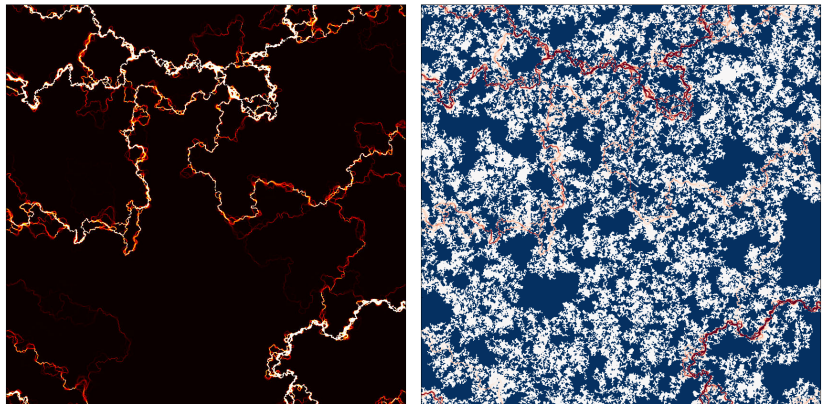
Creeping fluid transport



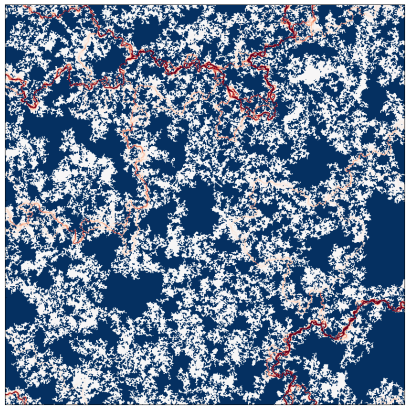
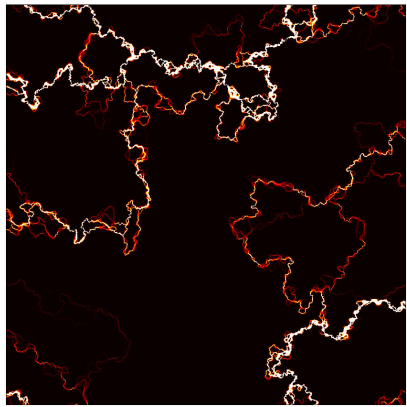
Creeping fluid transport



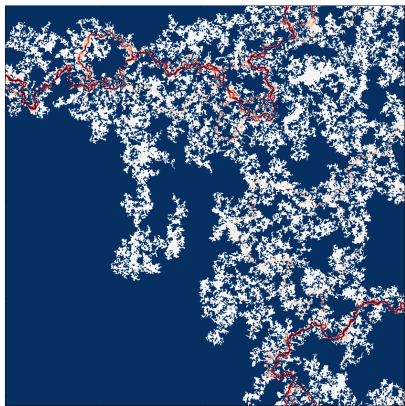
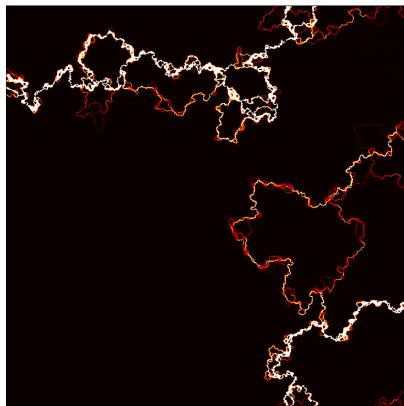
Creeping fluid transport



Creeping fluid transport



Creeping fluid transport



Contact area & trapped fluid

- Contact area does not conduct flow

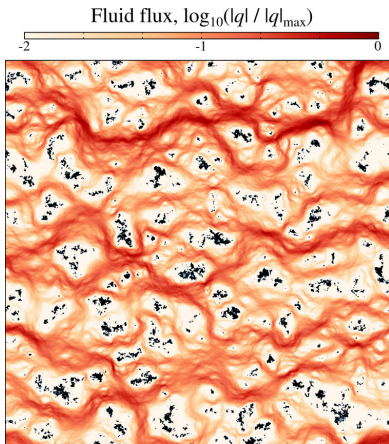


Fig. Fluid flux

Contact area & trapped fluid

- Contact area does not conduct flow

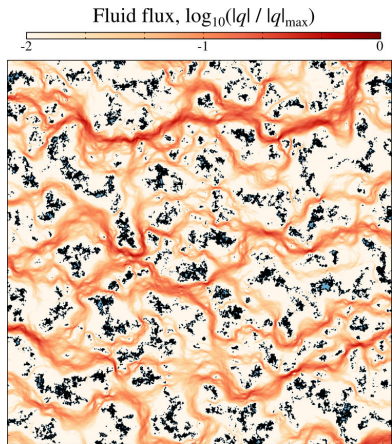


Fig. Fluid flux

Contact area & trapped fluid

- Contact area does not conduct flow

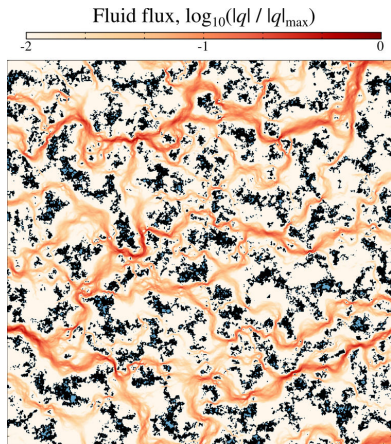


Fig. Fluid flux

Contact area & trapped fluid

- Contact area does not conduct flow

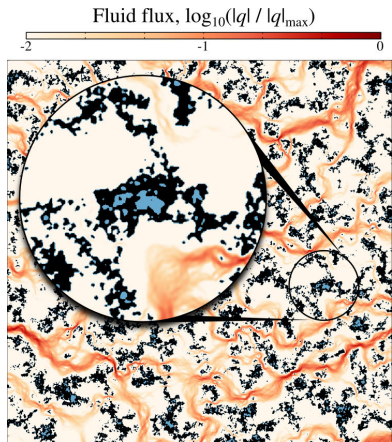


Fig. Fluid flux (zoom)

Contact area & trapped fluid

- Contact area does not conduct flow
- Islands of trapped fluid \equiv non-simply connected contact spots do not contribute to conduction
- Thus the effective transmissivity depends on the **effective contact area**:

$$A'_{\text{eff}} = A' + A'_t$$

A' is the contact area fraction

A'_t is the area of trapped fluid

- Effective medium transmissivity:

$$(1 - A') \int_0^{\infty} \frac{g^3 P(g)}{g^3 + K'_{\text{eff}} m_0^{3/2}} dg = \frac{1}{2}$$

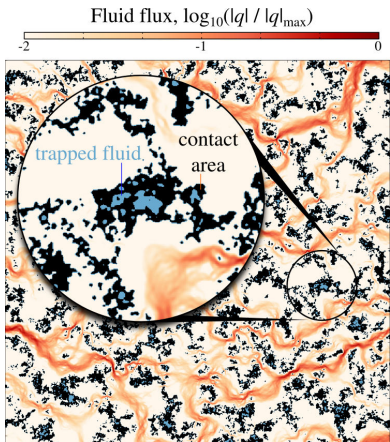


Fig. Fluid flux (zoom)

[1] Shvarts, Yastrebov. *Trapped Fluid in the Contact Interface*, JMPS:119 (2018)

Contact area & trapped fluid

- Contact area does not conduct flow
- Islands of trapped fluid \equiv non-simply connected contact spots do not contribute to conduction
- Thus the effective transmissivity depends on the **effective contact area**:

$$A'_{\text{eff}} = A' + A'_t$$

A' is the contact area fraction

A'_t is the area of trapped fluid

- Effective medium transmissivity:

$$(1 - A'_{\text{eff}}) \int_0^{\infty} \frac{g^3 P(g)}{g^3 + K'_{\text{eff}} m_0^{3/2}} dg = \frac{1}{2}$$

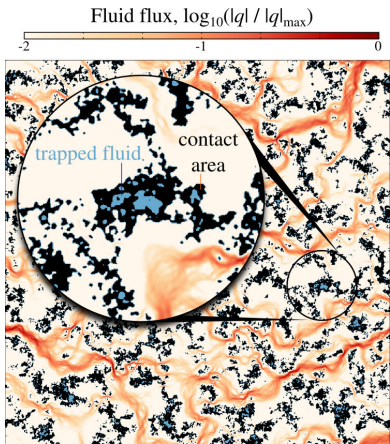


Fig. Fluid flux (zoom)

[1] Shvarts, Yastrebov. *Trapped Fluid in the Contact Interface*, JMPS:119 (2018)

Contact area & trapped fluid

- Contact area does not conduct flow
- Islands of trapped fluid \equiv non-simply connected contact spots do not contribute to conduction
- Thus the effective transmissivity depends on the **effective contact area**:

$$A'_{\text{eff}} = A' + A'_t$$

A' is the contact area fraction

A'_t is the area of trapped fluid

- Effective medium transmissivity:

$$(1 - A'_{\text{eff}}) \int_0^{\infty} \frac{g^3 P(g)}{g^3 + K'_{\text{eff}} m_0^{3/2}} dg = \frac{1}{2}$$

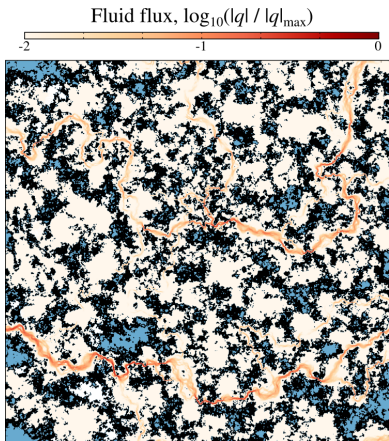


Fig. Fluid flux

[1] Shvarts, Yastrebov. *Trapped Fluid in the Contact Interface*, JMPS:119 (2018)

Contact area & trapped fluid

- Contact area does not conduct flow
- Islands of trapped fluid \equiv non-simply connected contact spots do not contribute to conduction
- Thus the effective transmissivity depends on the **effective contact area**:

$$A'_{\text{eff}} = A' + A'_t$$

A' is the contact area fraction

A'_t is the area of trapped fluid

- Effective medium transmissivity:

$$(1 - A'_{\text{eff}}) \int_0^{\infty} \frac{g^3 P(g)}{g^3 + K'_{\text{eff}} m_0^{3/2}} dg = \frac{1}{2}$$

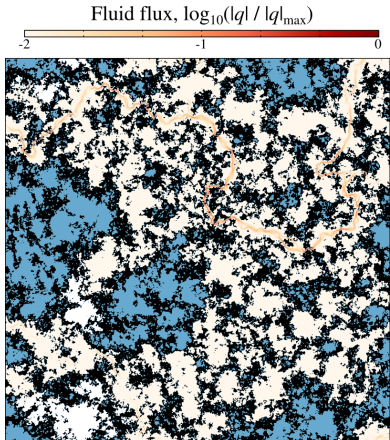


Fig. Fluid flux

[1] Shvarts, Yastrebov. *Trapped Fluid in the Contact Interface*, JMPS:119 (2018)

Contact area & trapped fluid

- Contact area does not conduct flow
- Islands of trapped fluid \equiv non-simply connected contact spots do not contribute to conduction
- Thus the effective transmissivity depends on the **effective contact area**:

$$A'_{\text{eff}} = A' + A'_t$$

A' is the contact area fraction

A'_t is the area of trapped fluid

- Effective medium transmissivity:

$$(1 - A'_{\text{eff}}) \int_0^{\infty} \frac{g^3 P(g)}{g^3 + K'_{\text{eff}} m_0^{3/2}} dg = \frac{1}{2}$$

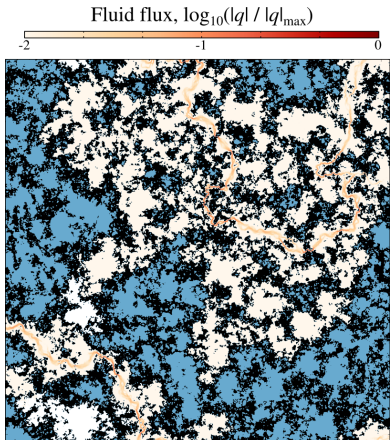
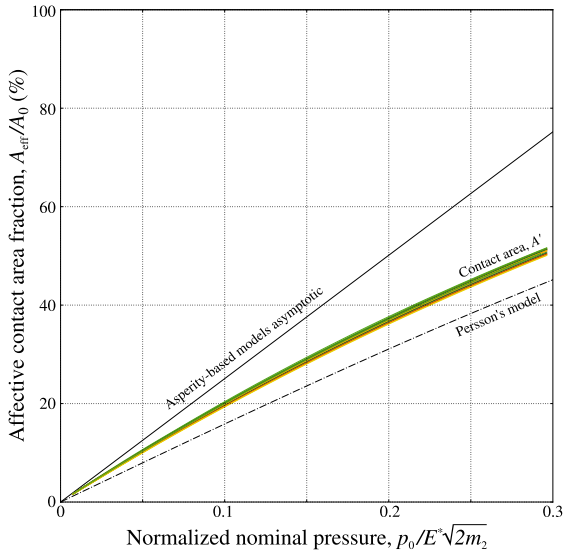


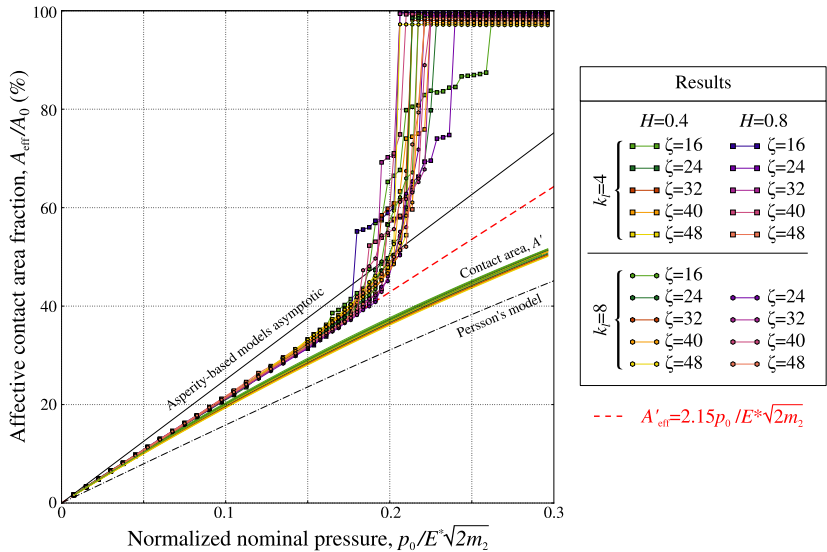
Fig. Fluid flux

[1] Shvarts, Yastrebov. *Trapped Fluid in the Contact Interface*, JMPS:119 (2018)

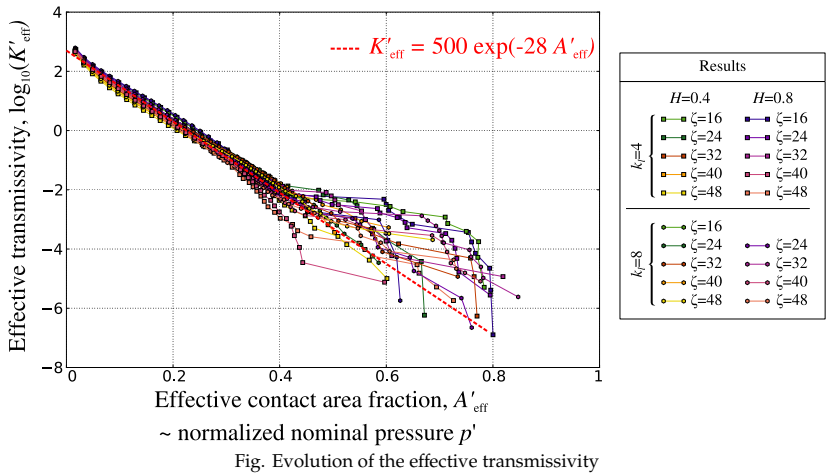
Effective contact area



Effective contact area



Normalized effective transmissivity



Effective transmissivity

- Effective area wrt load:

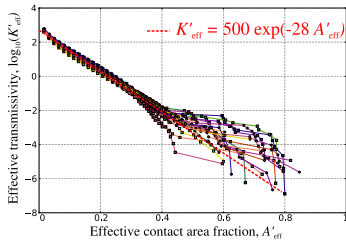
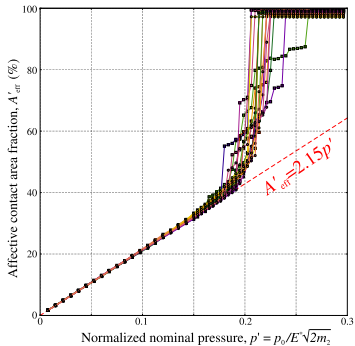
$$A'_{\text{eff}} \approx 2.15 p'$$

- Normalized load:

$$p' = p_0/E^* \sqrt{2m_2}$$

- Normalized effective transmissivity wrt effective area:

$$K'_{\text{eff}} \approx 500 \exp(-28 A'_{\text{eff}})$$



Effective transmissivity

- Effective area wrt load:

$$A'_{\text{eff}} \approx 2.15 p'$$

- Normalized load:

$$p' = p_0 / E^* \sqrt{2m_2}$$

- Normalized effective transmissivity wrt effective area:

$$K'_{\text{eff}} \approx 500 \exp(-28 A'_{\text{eff}})$$

- Recall:

$$K'_{\text{eff}} = -\frac{12\mu \langle q_x \rangle L}{m_0^{3/2} \Delta P_f}$$

- Express the mean flow:

$$\langle q_x \rangle = -\frac{K'_{\text{eff}} m_0^{3/2} \Delta P_f}{12\mu L}$$

- Finally:

$$\langle q_x \rangle \approx -\frac{41.7 \exp(-42.57 p_0 / E^* \sqrt{m_2}) m_0^{3/2} \Delta P_f}{\mu L}$$

Main result:

Mean flow¹ through contact of nominal area $L \times L$:

$$\langle q_x \rangle \approx -\frac{41.7 m_0^{3/2} \Delta P_f}{\mu L} \cdot \exp\left(-42.57 \frac{p_0}{E^* \sqrt{m_2}}\right)$$

μ is dynamic viscosity,

ΔP_f is the pressure drop between the inlet and the outlet,

p_0 is the nominal applied pressure,

E^* is the effective elastic modulus.

Roughness parameters:

m_0 is the variance of roughness,

$2m_2$ is the variance of roughness gradient.

¹far from percolation

Main result:

Mean flow¹ through contact of nominal area $L \times L$:

$$\langle q_x \rangle \approx -\frac{41.7 m_0^{3/2} \Delta P_f}{\mu L} \cdot \exp\left(-42.57 \frac{p_0}{E^* \sqrt{m_2}}\right)$$

μ is dynamic viscosity,

ΔP_f is the pressure drop between the inlet and the outlet,

p_0 is the nominal applied pressure,

E^* is the effective elastic modulus.

Roughness parameters:

m_0 is the variance of roughness,

$2m_2$ is the variance of roughness gradient.

Beyond the one-way coupling:

- Monolithic two-way FEM scheme coupling solid and fluid equations (thin flow, Reynolds equation) with contacts including islands of non-linear compressible fluid

¹far from percolation

General conclusion

The most critical assumption is the existence of the small wavelength cutoff

General conclusion

The most critical assumption is the existence of the small wavelength cutoff

- Fractal limit:

Let $\lambda_s \rightarrow 0$, then $m_2 \rightarrow \infty$ and $\forall p_0 < \infty, A' \rightarrow 0$

General conclusion

The most critical assumption is the existence of the small wavelength cutoff

- Fractal limit:

Let $\lambda_s \rightarrow 0$, then $m_2 \rightarrow \infty$ and $\forall p_0 < \infty, A' \rightarrow 0$

- Add some physics:

Let $\lambda_s \sim \text{\AA}$, then $m_2 < C < \infty$ and $\forall p_0 > 0, A' > 0$

General conclusion

The most critical assumption is the existence of the small wavelength cutoff

- Fractal limit:

Let $\lambda_s \rightarrow 0$, then $m_2 \rightarrow \infty$ and $\forall p_0 < \infty, A' \rightarrow 0$

- Add some physics:

Let $\lambda_s \sim \text{\AA}$, then $m_2 < C < \infty$ and $\forall p_0 > 0, A' > 0$

- But, at Å-scales, continuum mechanics and especially continuum contact^[1] do not work.

[1] Luan & Robbins. Nature 435 (2005).

General conclusion

The most critical assumption is the existence of the small wavelength cutoff

- Fractal limit:

Let $\lambda_s \rightarrow 0$, then $m_2 \rightarrow \infty$ and $\forall p_0 < \infty, A' \rightarrow 0$

- Add some physics:

Let $\lambda_s \sim \text{\AA}$, then $m_2 < C < \infty$ and $\forall p_0 > 0, A' > 0$

- But, at Å-scales, continuum mechanics and especially continuum contact^[1] do not work.

- Search for relevant physics that could justify $\lambda_s \gg \text{\AA}$.

- Candidates: plasticity (scale dependent), surface energy and adhesion, interaction potential.

[1] Luan & Robbins. Nature 435 (2005).



Thank you for your attention!
